Inorganic Chemistry

Article

pubs.acs.org/IC

Investigation of the Reactivity between a Ruthenium Hexacationic Prism and Biological Ligands

Lydia E. H. Paul,[†] Bruno Therrien,*[,‡] and Julien Furrer*[,†]

[†]Departement für Chemie und Biochemie, Universität Bern, Freiestrasse 3, CH-3012 Bern, Switzerland

[‡]Institut de Chimie, Université de Neuchâtel, Avenue de Bellevaux 51, CH-2000 Neuchâtel, Switzerland.

Supporting Information

ABSTRACT: The relative affinity of the cationic triangular metallaprism, $[(p\mathrm{CH_3C_6H_4Pr^i})_6\mathrm{Ru_6(tpt)_2(dhbq)_3}]^{6+}$ ($[\mathbf{1}]^{6+}$), for various amino acids, ascorbic acid, and glutathione (GSH) has been studied at 37 °C in aqueous solutions at pD 7, using NMR spectroscopy and electrospray ionization mass spectrometry (ESI-MS). The metallaprism $[\mathbf{1}]^{6+}$, which is constituted of six ($p\mathrm{CH_3C_6H_4Pr^i}$)Ru corners bridged by three 1,4-benzoquinonato (dhbq) ligands and connected by two 2,4,6tri(pyridin4yl)1,3,5-triazine (tpt) triangular panels, disassembled in the presence of Arg, His, and Lys, while it remains intact with Met. Coordination to the imidazole nitrogen atom in His or to the basic $\mathrm{NH/NH_2}$ groups in Arg and Lys displaces the dhbq and tpt ligands from the (*p*-cymene)Ru units, and subsequent coordination to the amino and carboxylato groups forms stable N,N,O metallacycles. The binding to amino acids proceeds rapidly, as determined by NMR spectroscopy. Interestingly, solutions of $[\mathbf{1}]^{6+}$ are able to catalyze oxidation of the thiol group of Cys and GSH to give the corresponding disulfides and of ascorbic acid to give the corresponding dehydroascorbic acid. Competition experiments with Arg, Cys, His, and Lys show the simultaneous formation of one single adduct, the (*p*-cymene)Ru-His complex, and oxidation of Cys to cystine. Furthermore, the (*p*-cymene)Ru-His complex formed upon the addition of His to $[\mathbf{1}][\mathrm{CF_3SO_3}]_6$ is able to oxidize Cys to cystine much more efficiently than $[\mathbf{1}]^{6+}$. These results provide evidence against interaction with proteins as process in the release of encapsulated guest molecules. Oxidation of Cys and GSH to give the corresponding disulfides may explain the *in vitro* anticancer activity of $[\mathbf{1}]^{6+}$.

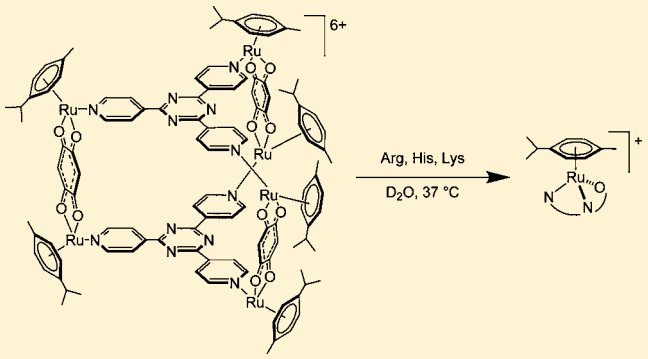

INTRODUCTION

The use of ruthenium complexes as anticancer agents was introduced and developed in the early 50s by Dwyer and co-workers,[1] but this research was mostly overlooked until the opportune discovery of cisplatin by Rosenberg and co-workers.[2] The subsequent developments in ruthenium anticancer drugs were mainly popularized by Clarke in the 1970s.[3] Indeed, ruthenium possesses several favorable chemical properties that indicate it may be a strong candidate to supplant platinum and to form a basis for rational anticancer drug design.[4] Interestingly, a number of ruthenium complexes have been found to display a significantly higher degree of selectivity toward cancerous cells than the leading commercially available platinum drugs,[2,5] resulting in reduced damage to healthy tissue.[6] Two inorganic Ru-based drugs, KP1019[7] and NAMI-A,[8] (Chart S1 in the Supporting Information, SI) have recently completed phase I clinical trials and have started (NAMI-A), or are expected soon to start a phase II study.[7,8] Despite their structural similarities, both compounds showed very different activities: NAMI-A appeared to be effective against lung metastases, whereas KP1019 showed activity against colon carcinomas. In the late 1980s, it was found that trans-Ru complexes were much more cytotoxic than their cis-counterpart, which is in stark contrast to the relative activities of the geometric isomers of Pt(II) complexes.[9] This feature already pointed to likely differences in the mechanisms of action of Ru(III) and Pt(II) complexes.

Numerous reviews on Ru anticancer drugs have tended to concentrate either on a single compound[7,10] or on a group of complexes,[11] and their different modes of reactivity in biological media.[12] Even though the mechanism of action and the biological targets of ruthenium drugs have not yet been fully elucidated, very recent evidence in the literature points to similarities in the mechanisms of action of various types of Ru anticancer complexes. For instance, specific antimetastatic activity, which was until recently regarded as a unique property of NAMI-A and its analogues, has also been demonstrated for RAPTA-type areneruthenium complexes (Chart S1 in the SI).[13] As with NAMI-A, the antimetastatic activity of areneruthenium complexes appears to be related to interactions with the extracellular matrix and the cell surface, rather than with DNA in the cell nucleus.[13]

More than 25 years ago, Maeda et al. addressed the potential value of macromolecular drugs and noted that increased

Received: October 11, 2011
Published: December 23, 2011

dx.doi.org/10.1021/ic2021935 | *Inorg. Chem.* 2012, 51, 1057−1067

permeability leads to higher uptake of large molecules and proteins.[14] Their observation was that the damaged lymphatic drainage of cancer cells leads to the selective retention of large molecules inside the cells.[15] This phenomena has been called the enhanced permeability and retention (EPR) effect. Therefore, large compounds are required in order to effectively exploit the size-selective uptake of drugs into tumor cells.[16]

The self-assembly of transition metal complexes with polydentate ligands to give discrete supramolecular assemblies, which has been first pioneered by Fujita,[17] appears very promising to exploit this EPR effect. So far, numerous two- and three-dimensional supramolecular structures incorporating square-planar transition metal ions have been synthesized and characterized.[18] These molecular architectures are very versatile and have been used in a large variety of applications such as gas storage, catalysis, and drug delivery.[17−19]

There has been therefore increasing interest in the anticancer properties of supramolecular areneruthenium assemblies during the past few years.[20] For instance, a series of trinuclear (*p*-cymene) Ru metallacycles connected with aminomethyl-substituted 3-hydroxy-2-pyridone ligands were evaluated *in vitro* against cancer and fibroblast cell lines. It was postulated that these water-soluble trinuclear complexes undergo fragmentation after uptake, thus giving rise to cytotoxic mononuclear complexes.[21] Stang et al. have recently synthesized new [2 + 2] metallarectangles with interesting *in vitro* cytotoxic properties for various human cancer cell lines.[20f] They have also synthesized hexanuclear areneruthenium-prismatic cages[20e,22] from which one showed a remarkable low micromolar activity (IC_{50} = 3.4 μM) on the A549 cell line.[20e]

We have recently synthesized a number of areneruthenium metalla-assemblies, in particular water-soluble hexacationic metallaprisms that form hexanuclear cages.[20d,23] Notably, these metallaprisms were capable of encapsulating planar Pt and Pd acetylacetonate complexes,[20a] as well as planar aromatic compounds of various sizes.[24] In these systems the encapsulated guest is stable, with the physical properties of the prism being retained following encapsulation. Interestingly, the metallaprism $[\mathbf{1}]^{6+}$ itself exhibits a remarkable activity (IC_{50} = 23 μM) against A2780 cancer cell lines, which increases with the encapsulation of planar Pt and Pd acetylacetonate complexes (IC_{50} = 12 and 1 μM, respectively) suggesting transport and leaching of the guest once inside the cell.[20a] However, for all cytotoxic areneruthenium metalla-assemblies investigated so far, very little is known about the mechanism of antitumor action, uptake, release of the guest, and the other biological processes.

Given the lack of information with metalla-assemblies, we report here a comparative study of the interactions of $[\mathbf{1}]^{6+}$ with various biological ligands. Since it was shown that $[\mathbf{1}]^{6+}$ can encapsulate biologically active guest molecules and can leach them once inside the cell,[20a] these experiments were undertaken to establish the nature of the species that are effectively transported into the cell, possible mechanisms of detoxification, as well as further information on the possible cellular target that may be related to its antitumor activity. The results showed that $[\mathbf{1}]^{6+}$ specifically interacts with the thiol groups of Cys and GSH, and with the side chain of His, Lys, and Arg. Remarkably, $[\mathbf{1}]^{6+}$ efficiently catalyzed oxidation of ascorbic acid, and the thiols Cys and GSH give dehydroascorbic acid and the corresponding disulfides, which may explain its *in vitro* anticancer activity. The reactions with His, Lys, and Arg formed stable decomposition products that have been fully characterized. Similarly to the mechanisms of action of numerous Ru-drugs investigated so far, our results strongly suggest that $[\mathbf{1}]^{6+}$ possesses a different mechanism of cancer cell cytotoxicity as compared to Pt-drugs.

EXPERIMENTAL SECTION

Material and Methods. Chemicals obtained from commercial suppliers were used as received and were of analytical grade; $RuCl_3 \cdot 3H_2O$ was obtained from Johnson Matthey; L-Ala, L-Arg, L-Cys, L-Gln, L-Gly, L-His, L-Lys, L-Met, L-Phe, L-Ser, and L-Trp were purchased from Acros; L-Asn, L-Asp, L-Glu, L-Ile, L-Leu, L-Pro, L-Thr, L-Tyr, and L-Val were purchased from Alfa Aesar; and L-ascorbic acid was purchased from Hänseler AG.

NMR data were acquired at a temperature of 310 K using a Bruker AvanceII 500 MHz NMR spectrometer equipped with an inverse dual channel (^{1}H, X) *z*-gradient probehead (BBI) or on a Bruker AvanceII 400 MHz NMR spectrometer equipped with an inverse dual channel (^{1}H, X) *z*-gradient probehead (BBI).

1D ^{1}H NMR data were acquired with 16−64 transients into 32k data points over a width of 12 ppm using a classical presaturation to eliminate the water resonance. A relaxation delay of 6 s was applied between transients.

2D ^{1}H−^{1}H NMR COSY data were acquired over a frequency width of 12 ppm in both F_2 and F_1 into 2k complex data points in F_2 (acquisition time = 213 or 170 ms) using 128 or 256 t_1 increments. A relaxation delay of 2 s between transients was used for all experiments. The data were recorded using 4 or 8 transients, depending on the samples. The water resonance was suppressed by means of a presaturation routine. A few ^{1}H 2D ROESY NMR data were recorded with mixing time of 200 ms (Tr-ROESY scheme[25]) using 128 transients, but were mostly unusable.

2D ^{1}H−^{13}C HSQC NMR data were acquired, with ^{13}C decoupling during the acquisition period, over an F_2 frequency width of 12 ppm into 2k complex data points (acquisition time = 213 or 170 ms). Transients (16−32) were accumulated for each of 196 t_1 increments over an F_1 frequency width of 180 ppm centered at 90 ppm. Phase-sensitive data were acquired in a sensitivity-improved manner using an echo−antiecho acquisition mode.

2D ^{1}H−^{13}C HMBC NMR data were acquired over an F_2 frequency width of 12 ppm into 2k complex data points (acquisition time = 213 or 170 ms). Transients (64−96) were accumulated for each of 196 t_1 increments over an F_1 frequency width of 200 ppm centered at 100 ppm. Phase-sensitive data were acquired in a sensitivity-improved manner using an echo−antiecho acquisition mode.

2D ^{1}H-DOSY NMR experiments were acquired with a standard pulsed-gradient stimulated echo (LED-PFGSTE) sequence containing bipolar gradients.[26] For all experiments, the airflow was increased to 670 L/min, and the NMR tube was spun. Experimental parameters were Δ = 100 ms (diffusion delay), τ = 1 ms (gradient recovery delay), and T = 5 ms (eddy current recovery delay). For each data set, 4k complex points were collected, and the gradient dimension was sampled by means of 32 experiments in which the gradient strength was linearly incremented from 1.0 to 50.8 G/cm. The gradient duration $\delta/2$ was adjusted to observe a near-complete signal loss at 50.8 G/cm. Typically, the $\delta/2$ delay was chosen in the 1.6−2.0 ms range. A 2 s recycle delay was used between scans for data shown. For each data set, the spectral axis was processed with an exponential function (3−5 Hz line broadening), and Fourier transform was applied to obtain 8k real points. The DOSY reconstruction was realized with 8k complex points in the detection dimension and with 256 points in the diffusion dimension. The number of scans ranged from 16 to 64 and was adapted to each sample. All NMR data were processed using Topspin (versions 2.1 or 3.0, Bruker Switzerland).

Mass spectrometric analyses were performed on a LTQ Orbitrap XL mass spectrometer (Thermo Fisher Scientific, Bremen, Germany), equipped with a nanoelectrospray ion source.

Stability in Aqueous Solution. In order to evaluate the stability of $[\mathbf{1}]^{6+}$ in aqueous solution, the metallaprism $[\mathbf{1}][CF_3SO_3]_6$ (2 mg) was dissolved in 0.6 mL of D_2O, and the sample was analyzed by ^{1}H NMR spectroscopy. To study a potential effect of the presence of

dx.doi.org/10.1021/ic2021935 | Inorg. Chem. 2012, 51, 1057−1067

chloride and other anions, we dissolved $[\mathbf{1}][CF_3SO_3]_6$ in 50 mM D_2O solutions of NaCl, KCl, KI, KF, and Na_2CO_3. In all cases, ^1H NMR spectra were recorded immediately after sample preparation, and every 2 h during 24 h.

Reactions with Biological Ligands Monitored by NMR Spectroscopy. If not otherwise specified, all binding experiments were carried out by mixing solutions of the metallaprism $[\mathbf{1}][CF_3SO_3]_6$ (2 mg) in 0.6 mL of D_2O with 10 equiv of the different ligands. Since $[\mathbf{1}][CF_3SO_3]_6$ is between 30 and 40 times heavier (M = 3345 g/mol) than the biological ligands considered and its solubility in water is about 4 mg/mL, the biological ligands could not been incubated with $[\mathbf{1}][CF_3SO_3]_6$ at ratios inferior to 6:1. All reactions were first monitored by 1D ^1H NMR spectra. 2D homonuclear $^1H-^1H$ and heteronuclear $^1H-^{13}C$ NMR experiments were recorded once steady state was confirmed in the ^1H NMR spectra. Preliminary experiments on $[\mathbf{1}]^{6+}$ and biological ligands were undertaken at pD = 7, i.e., close to the pH value of bloodstream, and at pD = 5.5, i.e., close the pH of cancer cells. The pD values of D_2O solutions were measured by use of a glass electrode and addition of 0.4 to the pH meter reading.[27] Minor differences were noticed between the two sets of NMR spectra, and the spectrum recorded at pD = 5.5 exhibited additional resonances near the original resonances of $[\mathbf{1}]^{6+}$ (Figure S37). A lower pD value seemed to initiate a reaction, probably because at pD = 5.5, the tpt moiety can be protonated. The resonances of His remained however unchanged, and the kinetic and the resulting adducts formed upon the addition of His were absolutely identical at both pD values. Therefore, all experiments presented in this work were undertaken at pD = 7. As our aim was to study the interactions between $[\mathbf{1}]^{6+}$ and biological ligands in conditions close to physiological conditions, oxygen was not excluded from the solutions. In addition, as preliminary experiments, we monitored by 1D and 2D NMR spectroscopy the interactions between $[\mathbf{1}]^{6+}$ and His in D_2O and in D_2O with 50 mM NaCl. Analysis revealed that the kinetics and the resulting adducts formed upon the addition of His were absolutely identical with or without 50 mM NaCl. The only difference in the spectra arose from the changes observed in the spectra of $[\mathbf{1}]^{6+}$ upon the addition of 50 mM NaCl presented in the Results and Discussion section. Therefore, for simplifying the analysis, all reactions were performed in D_2O. The ^1H and ^{13}C chemical shifts of free ascorbic acid, Arg, Cys, His, Lys, and GSH recorded in D_2O at 37 °C are given in Tables S1 and S2 in the SI.

Mass Spectrometry Studies on the Binding to Selected Biological Ligands. Stock solutions of $[\mathbf{1}][CF_3SO_3]_6$, Arg, Cys, His, Lys, and GSH (each 0.598 mM) were prepared in H_2O. Solutions of $[\mathbf{1}][CF_3SO_3]_6$ were incubated with the selected amino acid at a 1:6 molar ratio for 24 h at 37 °C. In order to follow the competitive reaction of $[\mathbf{1}]^{6+}$ with amino acids, a mixture $[\mathbf{1}]^{6+}$/Arg/Cys/His/Lys (ratio 1:6:6:6:6) was prepared and incubated for 24 h. The samples were analyzed in the positive ion mode with a voltage of +700 V applied to the glass emitter (New Objective, Woburn, MA). The tube lens was at +150 V, and the transfer capillary was held at 200 °C. Spectra were acquired in the FTMS mode over a range from m/z 200 to 2000 with a resolution of 100 000 at m/z 400. Calibration of the instrument was performed with ProteoMass LTQ/FTHybrid ESI positive mode calibration mix (Supelco Analytical, Bellefonte, PA). The Xcalibur software package (Xcalibur 2.0.7, Thermo Fisher Scientific) was used for instrument control and data processing.

RESULTS AND DISCUSSION

Synthesis and Characterization. The hexanuclear metallaprism $[\mathbf{1}][CF_3SO_3]_6$ (Chart 1) was prepared from the dinuclear complex $[(p\text{-cymene})_2Ru_2(dhbq)Cl_2]$ and tpt in the presence of silver triflate according to the literature method.[22,29] The ^1H NMR spectrum of $[\mathbf{1}]^{6+}$ in D_2O is fairly simple and contains a doublets at δ 8.56 and 8.58 assigned to the H_α and H_β of tpt, two doublets at δ 6.09 and 5.84 assigned to the p-cymene ring protons, one singlet at 5.99 assigned to the six isolated protons of dhbq, and one septet at δ 2.91, one singlet at δ 2.19,

Chart 1. Hexanuclear Metallaprism $[\mathbf{1}][CF_3SO_3]_6$

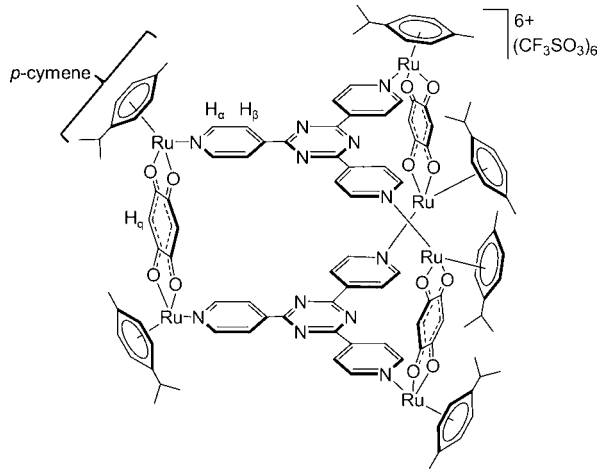

and one doublet at δ 1.35 for the p-cymene protons. The ^{13}C chemical shifts (obtained from $^1H-^{13}C$ HSQC and HMBC NMR spectra) were found at δ 183.7 (CO), 153.4 (CH_α), 144.3 (C_{tpt}), 124.4 (CH_β), 104.7 ($C_{p\text{-cym}}$), 102.0 (CH_q), 99.5 ($C_{p\text{-cym}}$), 83.7 ($CH_{p\text{-cym}}$), 81.3 ($CH_{p\text{-cym}}$), 30.8 ($CH(CH_3)_2$), 21.7 ($CH(CH_3)_2$), and 17.2 ($(CH_3)_{p\text{-cym}}$).

Stability in Aqueous Solution. In order to assess the stability of $[\mathbf{1}]^{6+}$ in solution, we first recorded the ^1H NMR spectra of $[\mathbf{1}]^{6+}$ dissolved in D_2O during 24 h. The ^1H NMR spectra showed no signal changes after 24 h at 37 °C, thus indicating that $[\mathbf{1}]^{6+}$ remains stable (Figure 1A). On the other hand, the addition of 50 mM NaCl seemed to initiate a reaction (Figure 1B). The same result was observed by using KCl instead of NaCl (Figure S2 in the SI). By using KF the reaction was much slower, and after 24 h the decrease in signal intensity of the original resonances was much less observable than with the salts containing chlorine.

In the presence of $[Cl^-]$, after 4 h, additional resonances appeared, and changes in the spectra were clearly observed. The intensity of the tpt resonances decreased whereas new resonances emerged adjacent to the original tpt resonances. The same phenomenon was observed for the resonances of p-cymene ligands. The NMR data suggest slow addition of $[Cl^-]$ after dissolution in aqueous environment. This might be because of either the increased electron density at the metal center or possible interactions between the nitrogen atoms of tpt and $[Cl^-]$. A DOSY spectrum showed that $[\mathbf{1}]^{6+}$ does not disassemble upon the addition of $[Cl^-]$, but rather that $[Cl^-]$ interacts/binds on tpt (Figure S3 in the SI). Indeed, the diffusion coefficient of $[\mathbf{1}]^{6+}$ upon the addition of $[Cl^-]$ was identical to the diffusion coefficient of $[\mathbf{1}]^{6+}$ in pure D_2O, thereby indicating no disassembling (Figure S3 in the SI). Finally, the addition of 50 mM Na_2CO_3 seemed to initiate another type of reaction (Figure S4 in the SI). Immediately after the dissolution of $[\mathbf{1}][CF_3SO_3]_6$ in a Na_2CO_3 solution, the ^1H NMR spectrum revealed the disappearance of the tpt resonances, as well as a strong decrease of the dhbq resonance's intensity and the appearance of a second set of resonances for the p-cymene group slightly upfield shifted. During the following 24 h the ratio between the two sets of p-cymene resonances increased to about 1:10. A DOSY spectrum (Figure S5 in the SI) showed that this new set of p-cymene resonances belongs to two new complexes, with a substantial lower molecular mass compared to complex $[\mathbf{1}][CF_3SO_3]_6$. Taken together, these results strongly

dx.doi.org/10.1021/ic2021935 | Inorg. Chem. 2012, 51, 1057–1067

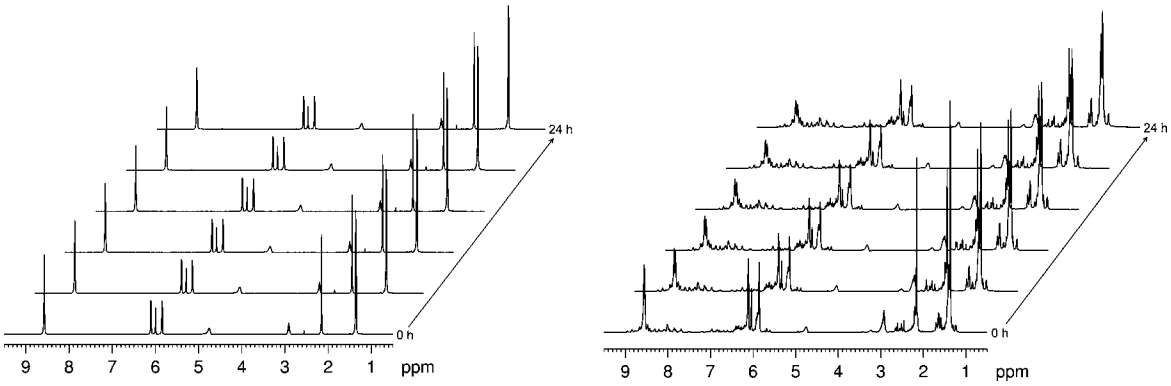

Figure 1. Stability of $[\mathbf{1}]^{6+}$ assessed by ^{1}H NMR spectra recorded during 24 h. Left: $[\mathbf{1}]^{6+}$ in D_2O. Right: $[\mathbf{1}]^{6+}$ in D_2O with the addition of 50 mM NaCl.

suggest that $[CO_3^{2-}]$ rapidly react with $[\mathbf{1}]^{6+}$ and displace tpt and dhbq which precipitate in water solutions, and only the *p*-cymene group remains bound to the Ru-atom. To validate this assumption, the precipitate was collected and dissolved in DMSO-d_6, and the resulting ^{1}H NMR spectrum confirmed the presence of tpt (Figure S6 in the SI). All results considered together, these measurements showed that the metallaprism $[\mathbf{1}]^{6+}$ remains stable for about 2 h upon the addition of chlorine salts, but disassemble rapidly upon the addition of carbonate.

REACTIONS WITH BIOLOGICAL LIGANDS

Reactions with Ascorbic Acid and Glucose. Currently, metallodrugs like cisplatin or carboplatin are administered intravenously, and hence, they may encounter a number of reactive biomolecules such as proteins in the bloodstream. Serum proteins like transferrin or albumin can play a divergent role either in delivery of metal based anticancer drugs to their cellular targets or in deactivating them even before reaching the target(s).[28] Therefore, the reactions of $[\mathbf{1}][CF_3SO_3]_6$ with various biological ligands, such as amino acids, ascorbic acid, glucose, and GSH, were investigated to gain insights into its reactivity to biomolecules and potential metabolization.

Ascorbic acid and glucose were chosen because of their concentrations in the bloodstream (the human body maintains the blood and cytosol ascorbic acid level between 20 to 40 μM and the blood glucose level between 3.6 and 5.8 mM), thus making them potential binding partners for metallodrugs. In the various NMR spectra recorded after 24 h, no changes for the resonances of $[\mathbf{1}]^{6+}$ and of glucose as compared to the resonances of $[\mathbf{1}]^{6+}$ and glucose alone in solution were observed (Figure S7 in the SI). On the other hand, directly after the addition of 6 equiv of ascorbic acid to a solution of $[\mathbf{1}][CF_3SO_3]_6$ the slow formation of a new species could be evidenced in the NMR spectra. The addition of ascorbic acid resulted in the appearance of new resonances at δ 4.20, 4.30, 4.61, and 4.79, adjacent to the resonances of ascorbic acid (δ 3.78, 4.10, and 4.99) (Figure 2). These new resonances increased over time, relative to the resonances of ascorbic acid, and, in agreement with the literature, were assigned to the arising formation of dehydroascorbic acid.[29] After 24 h, the spectra revealed that about 50% of ascorbic acid was oxidized to dehydroascorbic acid. Markedly, the ^{1}H and ^{13}C chemical shifts of $[\mathbf{1}]^{6+}$ remained essentially unaffected upon the addition of ascorbic acid, which led to the conclusion that ascorbic acid or dehydroascorbic acid does not form stable adducts with $[\mathbf{1}]^{6+}$. However, the resonances of tpt and dhbq were significantly

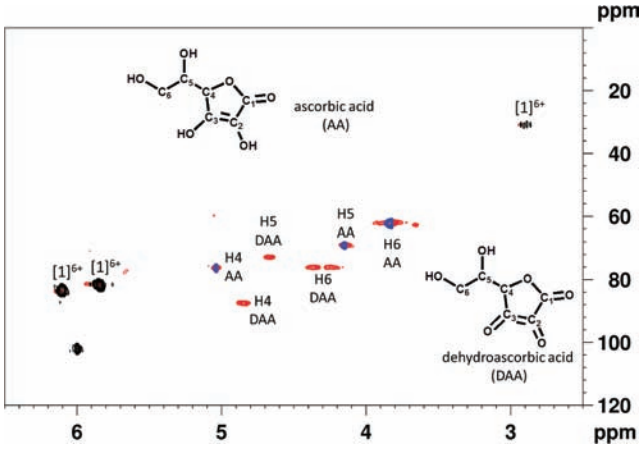

Figure 2. Excerpt of the 2D ^{1}H–^{13}C HSQC NMR spectrum of the mixture $[\mathbf{1}]^{6+}$/ascorbic acid (ratio 1:6) recorded after 24 h (red). For comparison, excerpts of the ^{1}H–^{13}C HSQC NMR spectra of $[\mathbf{1}]^{6+}$ (black) and free ascorbic acid (blue) were added.

broadened, which may indicate that ascorbic acid/dehydroascorbic acid slightly interacts with $[\mathbf{1}]^{6+}$, probably through $\pi-\pi$ interactions between the tpt/dhbq moieties and the double bonds of ascorbic acid/dehydroascorbic acid.

From these NMR experiments, it became apparent that $[\mathbf{1}]^{6+}$ can act as a catalyst for oxidation of ascorbic acid. This characteristic is known for Ru-complexes,[30] and it was for instance shown that NAMI-A can be reduced by a variety of agents present *in vivo*, including ascorbic acid.[31] The ability of $[\mathbf{1}]^{6+}$ to oxidize ascorbic acid might have an important biological significance, since ascorbic acid typically reacts with oxidants of the reactive oxygen species (ROS), usually hydroxyl radicals formed from hydrogen peroxide. These radicals are damaging to cells at the molecular level because of their possible interaction with nucleic acids, proteins, and lipids.

Reactions with Amino Acids and GSH. His, Met, and Cys are known to interact and to form adducts with many Ru-anticancer complexes,[32] and numerous reports can be found in the literature.[33] The study of the potential interactions with other amino acids such as Arg or Lys has not received much attraction, although there is experimental evidence that most of the amino acids bind to Ru-complexes.[32a,34] Since very little is known about the mode of action, uptake, and biological processes of $[\mathbf{1}][CF_3SO_3]_6$ and of metalla-assemblies in general, the reactions of $[\mathbf{1}][CF_3SO_3]_6$ with all natural amino acids were investigated. As expected, no reactions could be evidenced with

dx.doi.org/10.1021/ic2021935 | Inorg. Chem. 2012, 51, 1057–1067

most of the amino acids, and major changes in the NMR spectra were noticed only upon the addition of Arg, Cys, His, and Lys (Table S3 in the SI), showing that under the conditions studied coordination of either the carboxylato or the amino groups in amino acids to $[\mathbf{1}]^{6+}$ remains weak. The reactions observed could therefore be unequivocally attributed to the interactions of $[\mathbf{1}]^{6+}$ with the respective side chains (thiol of Cys, basic amine groups of Arg and Lys, and the imidazole group of His).

Reactions with Met. Rather surprisingly, no reaction occurred within 24 h with Met, and the resulting mixture was stable in solution for more than 72 h (Figure S8 in the SI). Met is known to undergo favorable binding interactions with metallodrugs, and in particular with platinum[35] and gold anticancer complexes.[35c,36] Ruthenium complexes also undergo favorable binding interactions with Met.[35c] For instance, Hartinger et al. showed that Met decomposed the areneruthenium complexes of 3-hydroxy-2(^{1}H)-pyridones within minutes. It was argued that the reactivity was because of the ability of Met to act as bidentate chelating ligands, with the thioether of Met and N1 or N3 atoms of the imidazole moiety.[37] A similar observation has been reported for related pyrone-derived complexes. It was also shown by Sadler et al. that the Ru(II) organometallic antitumor complex $[(\eta^6$-biphenyl)RuCl(en)$][PF_6]$ reacts with Met and gives rise to the adduct $[(\eta^6$biphenyl)Ru(*S*-L-MetH)-(en)$]^{2+}$, although only 27% of complex reacted.[33] Thus, unlike these Ru-complexes, $[\mathbf{1}]^{6+}$ does not form a stable adduct with Met.

Reactions with Cys. The interaction between $[\mathbf{1}]^{6+}$ and Cys in D_2O was monitored by 1D and 2D NMR spectroscopy as well as by ESI-MS measurements. The addition of 10 equiv of Cys resulted in the appearance of new resonances at δ 4.17, 3.46, and 3.27, adjacent to the resonances of Cys (δ Hα 4.01; δ Hβ 3.08, 3.14). These new ^{1}H resonances increased over time, relative to the resonances of Cys, and, in agreement with the literature, were assigned as arising from cystine.[38] After 48 h, the spectra revealed that oxidation of Cys to cystine was completed (Figure 3).

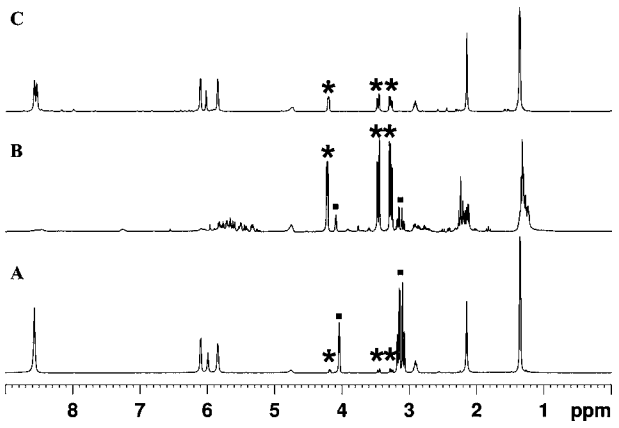

Figure 3. ^{1}H NMR spectra of $[\mathbf{1}]^{6+}$ directly after adding 10 equiv of Cys (**A**), after 24 h (**B**), and after 48 h (**C**). The conversion of Cys (■) into cystine (*) starts directly after the incubation and is completed after 48 h.

Formation of cystine was further confirmed by ESI-MS spectra of these solutions after 24 h of incubation, which showed peaks consistent with the presence of cystine (m/z observed 241.0, calculated for cystine 241.1). Interestingly, titrations with Cys revealed that the ^{1}H and ^{13}C chemical shifts of the αCH and βCH$_2$ groups of Cys were affected, but also the chemical shifts of $[\mathbf{1}]^{6+}$ (Figures 3 and S9 in the SI) suggesting that cystine forms stable adducts with $[\mathbf{1}]^{6+}$. However, formation of stable adducts with $[\mathbf{1}]^{6+}$ would imply the displacement of tpt and dhbq from the Ru-atom. Since both tpt and dhbq are completely insoluble in water, their ^{1}H resonances should not be visible in the NMR spectra. These resonances are however clearly visible (Figure 3). The DOSY spectrum confirmed that $[\mathbf{1}]^{6+}$ remains intact, since the diffusion coefficient of $[\mathbf{1}]^{6+}$ after 24 h of incubation with Cys remained identical to the diffusion coefficient of $[\mathbf{1}]^{6+}$ alone (Figure S10 in the SI). It should be however mentioned that many new additional resonances are visible in the various NMR spectra, especially in the regions of the aromatic *p*-cymene and dhbq. The exact origin of these additional resonances and the structure of the $[\mathbf{1}]^{6+}$ upon the addition of Cys were not further investigated. The stability of $[\mathbf{1}]^{6+}$ upon the addition of Cys was further confirmed by ESI-MS spectra recorded after 24 h of incubation, which showed peaks consistent with the presence of $[\mathbf{1}]^{6+}$ {m/z observed 687.3 and 966.4, consistent for $[\mathbf{1} + 3\ (CF_3SO_3)]^{3+}$ and $[\mathbf{1} + 2\ (CF_3SO_3)]^{4+}$} (Figure 4). From these ^{1}H NMR titration experiments, it became apparent that $[\mathbf{1}]^{6+}$ can act as a catalyst for oxidation of Cys to cystine.

Reactions with GSH. The stimulating results obtained with Cys prompted us to investigate whether $[\mathbf{1}]^{6+}$ would also be able to catalyze the conversion of GSH to oxidized GSH (GSSG). The thiol-containing tripeptide GSH (γ-Glu-Cys-Gly) is the major reducing agent in cells and is present in most cells in millimolar concentrations (0.5−10 mM). The catalytic conversion of GSH to GSSG may be directly related to anticancer activity, since cancer cells are known to have a higher GSH pool than healthy cells, and in all living cells, more than 90% of the total GSH pool is in the reduced form (GSH) and less than 10% exists in the disulfide form (GSSG). An increased of GSSG-to-GSH ratio is considered to be indicative of oxidative stress, which damages all components of the cell, including proteins, lipids, and DNA, and which may lead to apoptosis.[39]

In a pioneering study, Sadler and co-workers demonstrated that areneruthenium iodoazopyridine complexes act as catalysts for oxidation of the tripeptide GSH, thus suggesting to be at the origin of the observed anticancer activity.[40] However, incubation of 10 mM GSH with these complexes led to steady oxidation of only 4.6 mM GSH to GSSG, whereas oxidation of Cys to cystine is complete after 24 h with $[\mathbf{1}]^{6+}$ as catalyst. Our recently reported areneruthenium complex $[(p$-cymene$)_2$-$Ru_2(SC_6H_4$-p-$CH_3)_3]^+$ can also efficiently catalyze oxidation of GSH to give the corresponding GSSG, with turnover frequencies after 50% conversion (TOF_{50}) of about 8 h^{-1}.[41]

Similar NMR and ESI-MS experiments to those carried out with Cys were performed. GSH (6 equiv) was added to a solution of $[\mathbf{1}][CF_3SO_3]_6$ in D_2O, and the resulting mixture was first monitored by ^{1}H and ^{13}C NMR spectroscopy. Directly after mixing the peptide and the metallaprism $[\mathbf{1}][CF_3SO_3]_6$ the NMR spectra indicated no changes in the reaction mixture. However, after 24 h of incubation, significant changes in the NMR spectra could be observed. The resonances of tpt were significantly broadened whereas the resonances for dhbq disappeared completely (Figure S11 in the SI). Some resonances of GSH were shifted compared to free GSH, and subsequent analysis indicated a complete oxidation of GSH to GSSG, since the original Hα and Hβ resonances of Cys in GSH (δ Hα Cys 4.58; δ Hβ Cys 2.96, 3.01) were replaced by the characteristic

dx.doi.org/10.1021/ic2021935 | *Inorg. Chem.* 2012, 51, 1057−1067

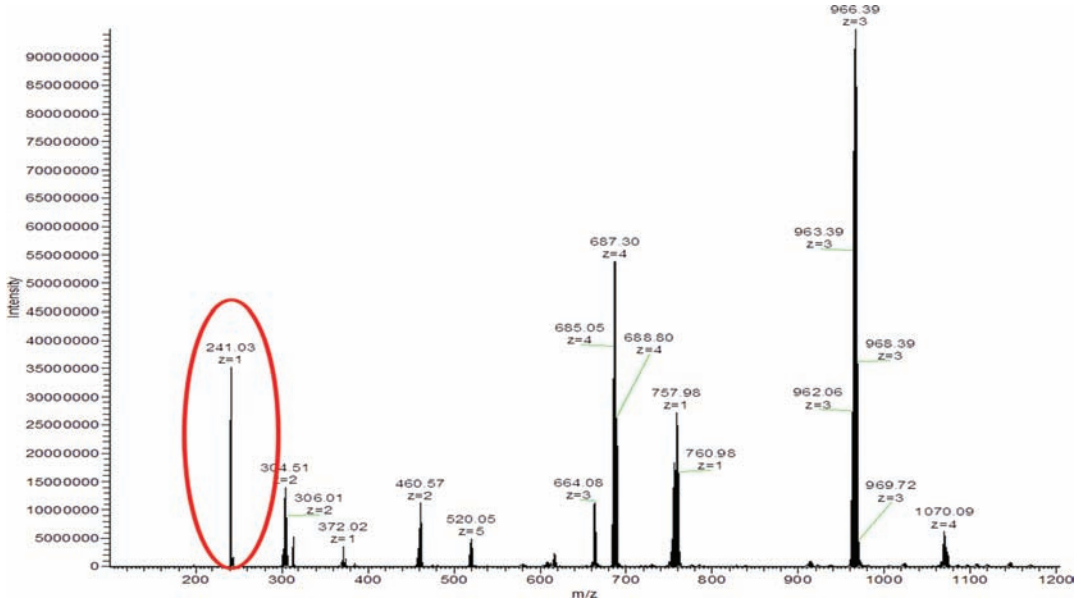

Figure 4. ESI-MS spectrum (positive mode) of $[\mathbf{1}][CF_3SO_3]_6$ and Cys (ratio 1:10) in H_2O recorded after 24 h. The peak consistent with the presence of cystine (m/z = 241.0) is highlighted.

Hα and Hβ resonances of GSSG (δ Hα Cys 4.82; δ Hβ Cys 3.07, 3.35).[42] Formation of GSSG was further confirmed by the ESI-MS spectrum of the mixture after 24 h of incubation, which shows peaks consistent with the presence of GSSG (m/z observed 613.16, calculated for GSSG 613.17) (Figure 6).

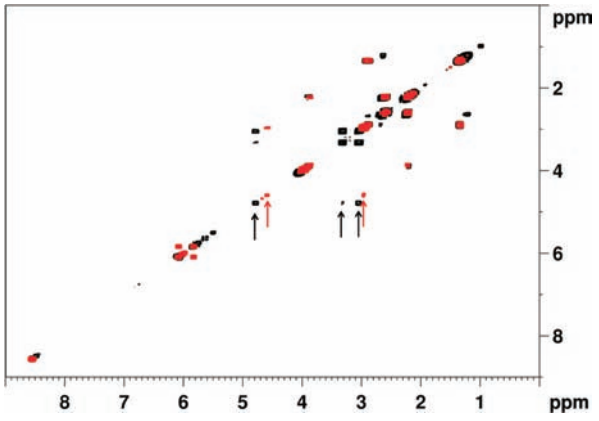

Figure 5. $^1H-^1H$ COSY NMR spectrum of $[\mathbf{1}]^{6+}$ after adding 6 equiv of GSH (red) and after 24 h (black). The shifts of the Hα and Hβ resonances of Cys (red arrows) are clearly visible (black arrows), indicating oxidation of GSH to GSSG.

The chemical shifts of $[\mathbf{1}]^{6+}$ were also significantly affected upon addition of GSH (Figure 5 and S11 in the SI). However, as pointed out before for Cys, formation of stable adducts with the (*p*-cymene)Ru units of $[\mathbf{1}]^{6+}$ could be ruled out, since the resonances of both tpt and dhbq were still visible in the various NMR spectra and the diffusion coefficient of $[\mathbf{1}]^{6+}$ after 24 h of incubation with GSH remained identical to the diffusion coefficient of $[\mathbf{1}]^{6+}$ alone (Figure S12 in the SI).

The complete oxidation observed for Cys and GSH in the presence of $[\mathbf{1}]^{6+}$ suggests that a partial oxidation of free thiols present in blood plasma must be considered as a possible mechanism of action. The major thiol source in blood plasma is the protein human serum albumin (HSA) which is present at approximately 0.63 mM concentration. This protein serves a number of important functions including the transport of drugs, metals, and hormones. Nevertheless, the only available thiol in HSA (Cys 34) is buried below the surface of the protein[43] and hence is much less accessible than the thiol group in Cys and GSH. Yet, the results shown here suggest that $[\mathbf{1}]^{6+}$ may interact with Cys 34 of HSA.

Reactions with Arg. Various NMR and ESI-MS experiments comparable to those performed for Cys and GSH were performed. The addition of Arg results in the immediate appearance of two new Hα resonances at δ 3.51 and 3.66 nearby the Hα of free Arg at δ 3.41. New resonances between δ 5.39 and δ 5.91 appeared as well, whereas the tpt resonances around δ 8.50 disappeared. As expected, after reaching equilibrium state, the resonances of free Arg at δ 3.41 (Hα); 1.60, 1.69 (Hβ); 1.69 (Hγ); and 3.19 (Hδ) remained also visible in the spectrum, and the ratio between the new Arg resonances and the resonances of free Arg is approximately 1:1:1, consistent with the hypothesis that one Arg reacts with one (*p*-cymene)Ru unit (Figure S13 in the SI). Curiously, the αCH and βCH_2 resonances of free Arg in the mixture (δ 3.41 and 1.60, 1.69, respectively) are downfield shifted compared to free Arg (δ 3.32 and 1.64, respectively). No ready explanation could be found to explain these shifts.

Upon coordination of Arg to the (*p*-cymene)Ru unit the *p*-cymene ring protons give four doublets, because of the epimerization of the chiral metal center and the presence of nonequivalent aromatic protons (Figure S13 in the SI). Concerning the behavior of coordinated Arg, only the ^1H and ^{13}C resonances of the αCH and βCH groups are significantly shifted compared to free Arg. Further analysis of the various 2D spectra revealed that the resonances at δ 3.51 and 3.66 arose from the Hα of coordinated Arg to $[\mathbf{1}]^{6+}$, whereas the resonances of tpt at δ 8.56 and the resonance of benzoquinone at δ 5.99 are missing in the spectra (Figures S13 and S14 in the SI). Therefore, taken together, these NMR spectra suggest that the reaction of $[\mathbf{1}]^{6+}$ with 10 equiv of Arg takes place within a few minutes with quantitative release of the tpt and dhbq ligands, because of the ability of the amino and carboxyl groups of

dx.doi.org/10.1021/ic2021935 | Inorg. Chem. 2012, 51, 1057–1067

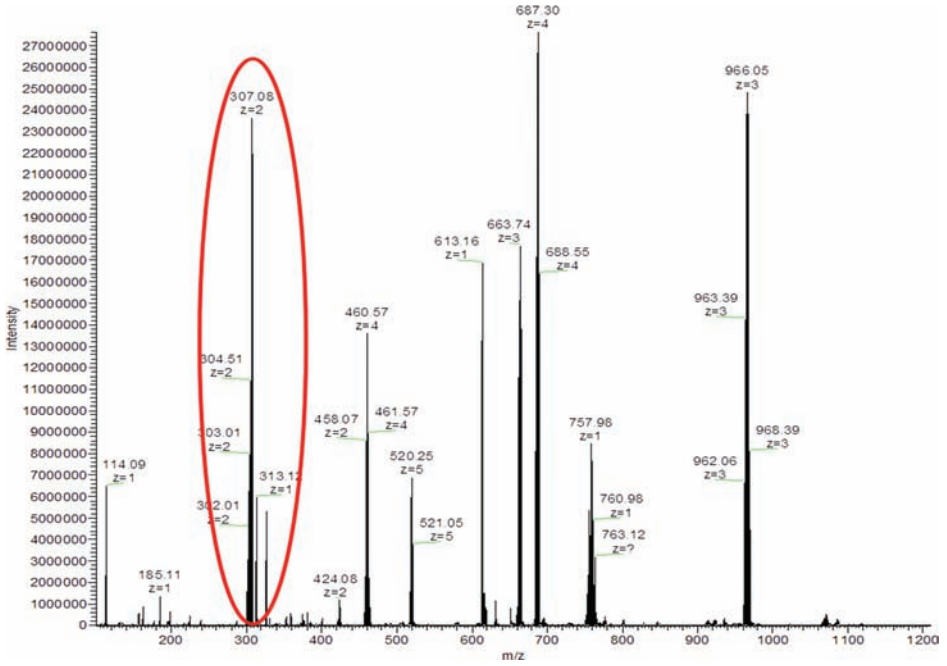

Figure 6. ESI-MS spectrum of $[\mathbf{1}][CF_3SO_3]_6$ and GSH (ratio 1:6) in H_2O recorded after 24 h. The peak consistent with the presence of GSSG (m/z = 307.1) is highlighted.

Arg to replace the N- and O-atoms of tpt and dhbq on the (*p*-cymene)Ru unit.

As a plausible mechanism, Arg may first coordinate to the Ru atom via one of the basic NH_2 group of the side chain inducing the quantitative release of the tpt moiety. Through this first coordination, the two Ru−O bonds between the Ru atom and dhbq are released by the carboxylato and the amino groups of Arg which can act as second and third ligands, thus forming a N,N,O chelate adduct (Chart 2). Formation and structural

Chart 2. Suggested (*p*-Cymene)Ru-Arg Chelate Complexes Obtained upon the Addition of Arg to $[\mathbf{1}]^{6+}$

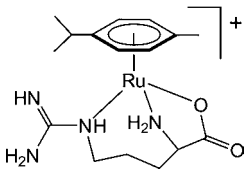

characterization of such areneruthenium metallacycles with *α*-amino acids have already been described.[34,44] The ability of the amino and carboxylato groups of Arg to replace the O-atoms of dhbq on the Ru atom offers the possibility of obtaining two distinct chiral adducts.[34,44] It has been already widely demonstrated that the various bond lengths and angles in areneruthenium complexes significantly deviate from an ideal tetrahedron.[45] Therefore, the two N,N,O and N,O,N chelate adducts are intrinsically chiral, which explains the occurrence of two distinct ^{1}H and ^{13}C resonances for the *α*CH and *β*CH groups in the observed complexes. Curiously, the ^{1}H and ^{13}C resonances of the *p*-cymene ring did not exhibit the expected two sets of four resonances, characteristic upon addition of *α*-amino acids to $[RuCl_2(arene)]_2$.[44] Formation of the chelate adducts was further supported by the 2D ^{1}H−^{13}C HMBC NMR spectrum (Figure S15 in the SI) which showed that the carbonyl resonances of these adducts are upfield shifted by 10 ppm compared to the carbonyl resonance of free Arg.

To further support these assumptions, ^{1}H DOSY NMR experiments were performed. As can be seen, the DOSY spectrum of the mixture $[\mathbf{1}]^{6+}$/Arg exhibits two sets of resonances, which correspond to molecules of different sizes (Figure 7). The resonances belonging to the smallest molecule

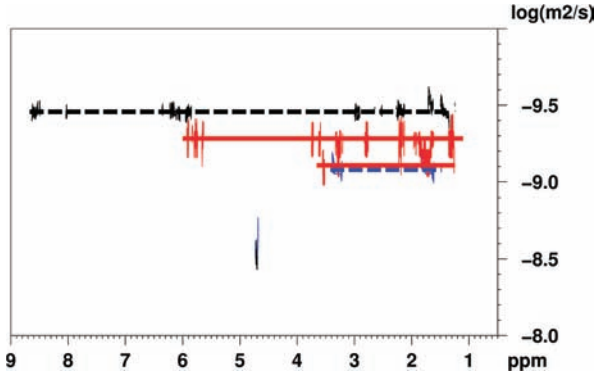

Figure 7. 2D ^{1}H DOSY NMR spectrum of the mixture Arg/$[\mathbf{1}]^{6+}$ (ratio 10:1, red) recorded after 36 h, as well as superimposed 2D ^{1}H DOSY NMR spectra of $[\mathbf{1}]^{6+}$ (black) and Arg (blue) for comparison.

can be attributed to free Arg (lower red line, Figure 7), while the other set of resonances belongs to the newly formed chelate adducts obtained in solution upon the addition of Arg to $[\mathbf{1}]^{6+}$ (upper red line, Figure 7). Compared to $[\mathbf{1}]^{6+}$ (black line, Figure 7), the DOSY spectrum clearly shows that this new (*p*-cymene)Ru-Arg adduct is smaller than $[\mathbf{1}]^{6+}$ alone, thus confirming the quantitative release of the tpt and dhbq ligands upon the addition of Arg observed in the various 1D and 2D NMR spectra.

Formation of the (*p*-cymene)Ru-Arg complex could be confirmed by ESI-MS measurements. The ESI-MS spectrum recorded on the mixture of $[\mathbf{1}]^{6+}$ with Arg exhibited a peak at

dx.doi.org/10.1021/ic2021935 | *Inorg. Chem.* 2012, 51, 1057−1067

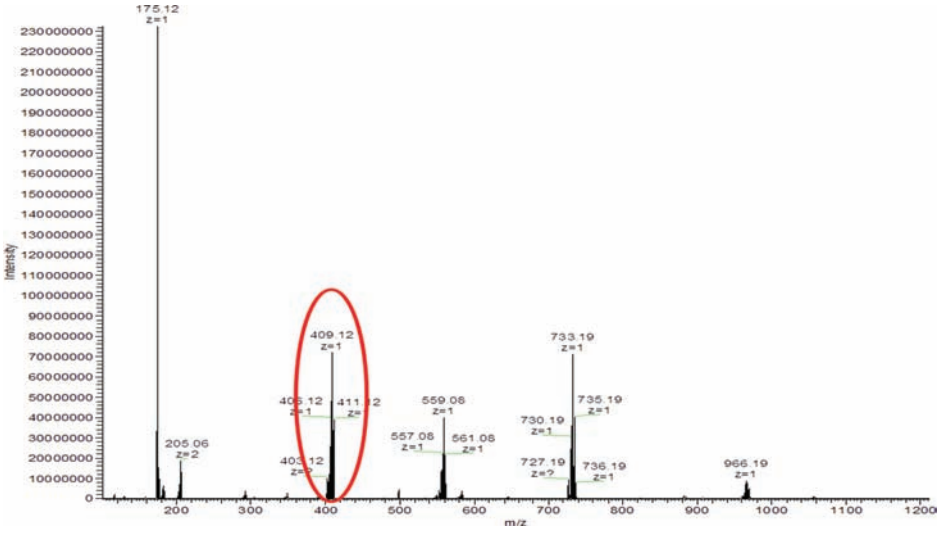

Figure 8. ESI-MS spectrum (positive mode) of the mixture $[\mathbf{1}]^{6+}$:Arg (ratio 1:10) in H_2O, recorded after 48 h. The peak consistent with the presence of the newly formed adduct [(*p*-cymene)Ru-Arg + H]$^+$ is highlighted.

m/*z* 409.1 which can be assigned to the adduct [(*p*-cymene)-Ru-Arg + H]$^+$. In addition, the peak at *m*/*z* 175.1 belonging to free Arg could also be found in the spectrum (Figure 8).

Reactions with Lys. Figure S16 shows the ^{1}H NMR spectra obtained before and after the addition of 10 equiv of Lys into a solution of $[\mathbf{1}]^{6+}$ in D_2O. As observed with Arg, the *p*-cymene ring protons exhibit four doublets between δ 5.64 and 5.91 upon coordination of Lys to (*p*-cymene)Ru units. As expected, the resonances of free Lys at δ 3.65 (Hα); 1.39, 1.46 (Hβ); 1.68 (Hγ); 1.83 (Hδ); and 2.98 (Hε) are also visible in the spectra (Figure S16 and S17). A small signal appears at δ 3.49 nearby the Hα of Lys suggesting formation of an adduct by the addition of Lys to $[\mathbf{1}]^{6+}$. In addition, the 2D ^{1}H−^{13}C HSQC NMR spectrum reveals that two adducts are actually formed, since the Hα resonance at δ 3.65 is correlated to two distinct Cα resonances, at δ 54.7 and 62.8, respectively (Figure S17 in the SI). As observed with Arg, the αCH and βCH$_2$ resonances of free Lys in the mixture (δ 3.65 and 1.39, 1.46, respectively) are shifted compared to free Lys (δ 3.42 and 1.72, 1.74, respectively).

2D spectra as well as a DOSY spectrum showed that the reaction of $[\mathbf{1}]^{6+}$ with 10 equiv of Lys takes place within minutes with quantitative released of the tpt ligands, again possibly because of the ability of the NH group of Lys to replace the N-atoms of tpt on the Ru atom. Also, the dhbq seems to be replaced quantitatively by Lys, since its typical resonances could not be identified in the ^{1}H as well as in the ^{1}H−^{13}C HSQC NMR spectra (Figure S17 in the SI). As found before for Arg, only the ^{1}H and ^{13}C chemical shifts of the αCH and of the carbonyl groups were significantly shifted upon coordination of Lys to $[\mathbf{1}]^{6+}$ (Figures S17 and S18 in the SI), therefore suggesting that Lys is bound to the Ru atom via the carboxylato and the amino groups to form the same type of N,N,O chelates (Chart 3).

As can be seen in the DOSY spectrum (Figure 9), the $[\mathbf{1}]^{6+}$/Lys mixture exhibits two sets of resonances, which can be correlated to molecules of different sizes. The resonances belonging to the smallest molecule can be attributed to free Lys (lower red line, Figure 9), while the other set of resonances belongs to the newly formed chelate adducts upon the addition of Lys to $[\mathbf{1}]^{6+}$ (upper red line, Figure 9). As observed for Arg, the DOSY spectrum clearly indicates that the molecular mass of

Chart 3. Suggested (*p*-Cymene)Ru-Lys Chelate Complex Obtained upon the Addition of Lys to $[\mathbf{1}]^{6+}$

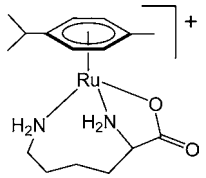

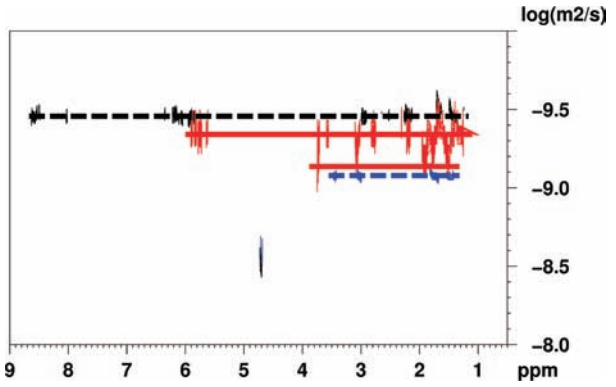

Figure 9. 2D ^{1}H DOSY NMR spectrum of the mixture Lys/$[\mathbf{1}]^{6+}$ (ratio 10:1, red) recorded after 24 h, as well as superimposed 2D ^{1}H DOSY NMR spectra of $[\mathbf{1}]^{6+}$ (black) and Lys (blue) for comparison.

the chelate adducts is significantly inferior to that of $[\mathbf{1}]^{6+}$ alone (black line, Figure 9), which confirms the quantitative release of the tpt and the dbhq ligands upon the addition of Lys observed in the various 1D and 2D NMR spectra.

Formation of the new adducts could also be confirmed by ESI-MS measurements. The ESI-MS spectrum recorded on the mixture of $[\mathbf{1}]^{6+}$ with Lys exhibited a peak at *m*/*z* 381.11 which can be assigned to the newly formed adduct [(*p*-cymene)Ru-Lys + H]$^+$. In addition, the peak at *m*/*z* 147.11 which belongs to free Lys could also be found in the spectrum (Figure S19 in the SI).

Reactions with His. Figure 10 shows the ^{1}H NMR spectra obtained after the addition of 10 equiv of His into a solution of $[\mathbf{1}][CF_3SO_3]_6$ in D_2O. As observed for Arg and Lys, the

dx.doi.org/10.1021/ic2021935 | *Inorg. Chem.* 2012, 51, 1057−1067

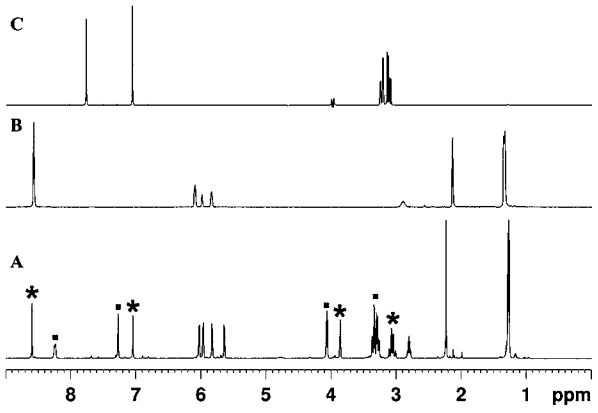

Figure 10. ^{1}H NMR spectra of $[\mathbf{1}]^{6+}$ and 10 equiv His recorded after 24 h (**A**), of $[\mathbf{1}]^{6+}$ (**B**), and of free His (**C**). The resonances of free His are indicated by small black solid squares, and the resonances of coordinated His by *.

p-cymene ring protons gave four doublets upon coordination of His to the Ru atom, thus once again suggesting breakage of the hexacationic metallaprism. The addition of His also results in the appearance of new resonances at δ 3.77, 2.94, and 3.01 near the resonances of free His, as well as new resonances at δ 7.19 and 8.50. The resonances of free His at δ 3.97 (Hα); 3.20, 3.27 (Hβ); 8.16 ($H2_{imidazole}$); and 7.19 ($H4_{imidazole}$) are also visible in the spectrum after reaching equilibrium, and the ratio between the new His resonances and the resonances of free His is approximately 6:4, suggesting that each (*p*-cymene)Ru unit reacts with one His.

Analysis of the various 2D spectra reveals that the resonances between δ 8.50 and 6.96 arose from coordinated His to $[\mathbf{1}]^{6+}$ and free His, whereas the resonances of tpt and of dhbq are again not visible in the spectra (Figure S20 in the SI). These findings also suggest, as found for Arg and Lys, that the reaction of $[\mathbf{1}]^{6+}$ with 10 equiv of His takes place with quantitative release of the tpt ligand, possibly due to the ability of N(3) to replace the N-atoms of tpt on the Ru atom (Chart 4). The 2D

Chart 4. Suggested (*p*-Cymene)Ru-His Chelate Complex Obtained upon the Addition of His to $[\mathbf{1}]^{6+}$[a]

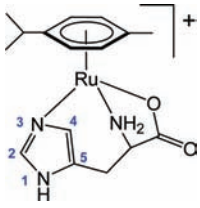

[a]The numbering of the imidazole group used in the text is indicated.

^{1}H−^{13}C HMBC NMR spectrum (Figure S21 in the SI) confirms formation of a chelate adduct, since the carbonyl resonance is downfield shifted by more than 10 ppm as compared to the carbonyl resonance of free His. In support of these findings, the DOSY NMR spectrum of the mixture $[\mathbf{1}]^{6+}$/His exhibits two different sets of diffusion coefficients, which, according to the other NMR spectra, belong to free His and to the newly formed chelate complex (Figure S22 in the SI). Interestingly, in contrast to Arg and Lys, which formed two chelate adducts with $[\mathbf{1}]^{6+}$, only one new resonance for the αCH group is observed in the NMR spectra, suggesting either formation of one single adduct, or that the ^{1}H and ^{13}C resonances of the αCH group resonate exactly at the same frequency in the two adducts. It seems however more likely that the imidazole group of His, being much less flexible than the alkyl chains of Arg and Lys, prevents formation of two adducts.

These findings are supported by the ESI-mass spectrum obtained after mixing $[\mathbf{1}][CF_3SO_3]_6$ and His (ratio 1:10) in which the peak at m/z 390.1 was assigned to [(*p*-cymene)Ru-(His) − H] . The peak at m/z 156.1 is assigned to free His. The presence of free tpt m/z 313.1 could also be evidenced (Figure S23 in the SI).

COMPETITION EXPERIMENTS

In order to test the relative affinity of $[\mathbf{1}]^{6+}$ for the thiol group of Cys compared to other potential coordinating ligands present in the amino acid side-chains, competition experiments were carried out between the amino acids Arg, Lys, His, and Cys. NMR titration experiments are performed in which 6 equiv of each amino acid is added to a solution of $[\mathbf{1}][CF_3SO_3]_6$ in D_2O. After reaching the equilibrium, the NMR spectra show again evidence that Cys was partially oxidized to cystine. The resonances of both the tpt or dhbq moieties are absent from the 1D and 2D spectra, which suggest a coordination of at least one amino acid to $[\mathbf{1}]^{6+}$. Analysis of the ^{1}H and HSQC NMR spectra (Figures 11 and S24 in the SI) showed the presence of

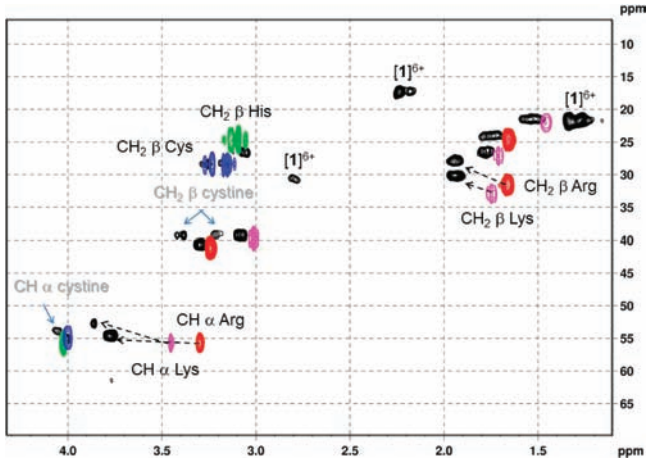

Figure 11. Aliphatic part of the ^{1}H−^{13}C HSQC NMR spectrum of the mixture $[\mathbf{1}]^{6+}$/Arg, Cys, His, and Lys in D_2O (ratio 1:6:6:6:6) recorded after 24 h (black contours). The aliphatic parts of the ^{1}H−^{13}C HSQC NMR spectra of Arg, red contours; Cys, blue contours; His, green contours; and Lys, magenta contours, were added for comparison. The resonances of cystine are indicated by plain blue arrows, and the low-field shifts of the αCH and βCH of Arg and Lys by dashed black arrows.

free Arg, Cys, His, and Lys, as well as of cystine and coordinated His (Figure S25 in the SI). In this competition experiment, the same shift of the αCH and βCH resonances of free Arg and Lys in the mixture compared to the free components is also observed.

These findings are further confirmed by the ^{1}H DOSY NMR spectrum (Figure S26 in the SI), which exhibits four distinct diffusion coefficients, corresponding to free His, free Arg, Cys, and Lys, the adduct (*p*-cymene)Ru-His, and $[\mathbf{1}]^{6+}$ upon the addition of Cys, respectively. The NMR results could be confirmed by ESI-MS experiments. The ESI-mass spectrum of the mixture $[\mathbf{1}]^{6+}$/Arg, Cys, His and Lys (ratio 1:6:6:6:6) in H_2O, recorded after 24 h (Figure S27 in the SI) exhibits peaks at m/z = 175.1, m/z = 156.1, m/z = 147.11, and m/z = 390.1,

dx.doi.org/10.1021/ic2021935 | Inorg. Chem. 2012, 51, 1057−1067

consistent with Arg, His, Lys, and to the adduct complex [(*p*-cymene)Ru-His + H]$^+$, respectively.

Interestingly, oxidation of Cys to cystine still occurs in the presence of the three other amino acids, suggesting that only the (*p*-cymene)Ru or (*p*-cymene)Ru-His moiety is required for catalyzing this reaction. To test this hypothesis, a further competition experiment was carried out: by adding 10 equiv of His to a solution of $[\mathbf{1}][CF_3SO_3]_6$ in D_2O, and after reaching the equilibrium, 6 equiv of Cys was added directly to the mixture containing the (*p*-cymene)Ru-His complex. Then addition of 6 equiv of Cys results in the appearance of the resonances at δ 4.17, 3.46, and 3.27 corresponding to cystine, while the original resonances of Cys (δ Hα 4.01; δ Hβ 3.08, 3.14) are now absent in the spectra (Figure 12).

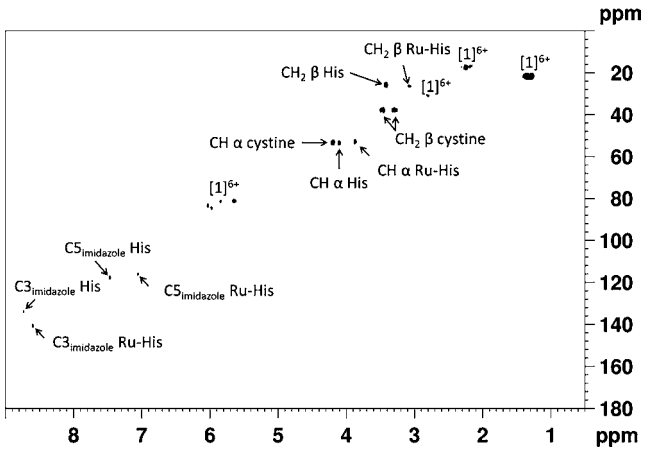

Figure 12. ^{1}H−^{13}C HSQC NMR spectrum of the mixture $[\mathbf{1}]^{6+}$/His (ratio 1:10) with a subsequent addition of 6 equiv Cys recorded after 24 h in D_2O.

These results demonstrate that the adduct complex (*p*-cymene)Ru-His is able to catalyze oxidation of Cys to cystine. The conversion seems to be even more effective using the (*p*-cymene)Ru-His complex compared to $[\mathbf{1}]^{6+}$, and is as good as with the areneruthenium complex $[(p\text{-cymene})_2Ru_2(SC_6H_4\text{-}p\text{-}CH_3)_3]^+$, which can convert Cys to cystine with turnover frequencies after 50% conversion of about 8 h^{-1}.[41]

CONCLUSIONS

The focus of this research was to establish the relative affinity of $[\mathbf{1}]^{6+}$ for biological ligands in physiological conditions, and therefore to predict the complexes or adducts that would most likely form in biological media, including blood plasma. No evidence for coordination to $[\mathbf{1}]^{6+}$ of the carboxylato or amino groups in most of the amino acids was detected using ^{1}H NMR spectroscopy. In contrast, the imidazole group of His, the basic amino groups of Lys and Arg, were shown to break the hexanuclear metallaprism $[\mathbf{1}]^{6+}$, and to coordinate to the (*p*-cymene)Ru unit, thus generating various stable adducts. Interestingly, these results suggest that Arg, His, and Lys act as chelating ligands for the Ru atom. Most probably, His coordinates first to Ru via N(3) of the imidazole ring, whereas Arg and Lys coordinate first to Ru via the basic NH groups of the side chain. This first coordination induces the quantitative release of the tpt moiety, which activates the two Ru−O bonds between the Ru atom and dhbq. The carboxylato and the amino groups can thus act as second and third ligands, thus forming a stable N,N,O chelate adduct with the remaining (*p*-cymene)Ru moiety. On the other hand, our results show that $[\mathbf{1}]^{6+}$ remains inert in the presence of glucose, and strongly support the fact that it can act as a precatalyst for oxidation of ascorbic acid to dehydroascorbic acid, of Cys to cystine and of GSH to GSSG, which might explain its good cytotoxicity (IC_{50} = 23 μM) against A2780 cancer cell lines.

The coordination chemistry of $[\mathbf{1}]^{6+}$ contrasts with the coordination chemistry of some other Ru-complexes, which showed strong interaction with Met,[33,37] and weak, labile coordination to carboxylate groups in amino acids.[46] The results reported in this study strongly suggest that $[\mathbf{1}]^{6+}$ will preferentially react to amino groups, while simultaneously oxidizing ascorbic acid, Cys, and GSH to dehydroascorbic acid, cystine, and GSSG. Thus, serum proteins like serum albumin and transferrin are attractive targets for $[\mathbf{1}]^{6+}$ and more generally for areneruthenium metalla-assemblies. The coordination mode of $[\mathbf{1}]^{6+}$ is distinct from the coordination chemistry of other cytotoxic Ru-complexes, and the results are consistent with other studies that do not necessarily implicate Ru-DNA adducts in the mechanism of action. Further studies to determine the coordination of nucleotides and DNA to areneruthenium metalla-assemblies will be useful in further establishing their mechanism of action. Furthermore, our results show that the complex (*p*-cymene)Ru-His formed upon the addition of His to $[\mathbf{1}][CF_3SO_3]_6$ can very efficiently oxidize Cys to cystine. Further studies to determine the ability of (*p*-cymene)Ru-(amino acid) complexes to oxidize GSH to GSSG will also be useful in understanding the mechanism of action of this class of compounds.

ASSOCIATED CONTENT

Supporting Information

Structures of NAMI-A, KP1019, and RAPTA compounds; tables of ^{1}H and ^{13}C chemical shifts; additional NMR and ESI-MS spectra; experimental details for characterization of the various adducts. This material is available free of charge via the Internet at http://pubs.acs.org.

AUTHOR INFORMATION

Corresponding Author

*E-mail: julien.furrer@dcb.unibe.ch (J.F.); bruno.therrien@unine.ch (B.T.).

ACKNOWLEDGMENTS

J.F. thanks the Swiss National Science Foundation (Grant 200021-131887) for financial support. A generous loan of ruthenium chloride hydrate from the Johnson Matthey Technology Center is gratefully acknowledged.

REFERENCES

(1) Dwyer, F. P.; Gyarfas, E. C.; Rogers, W. P.; Koch, J. H. *Nature* **1952**, *170*, 190.
(2) Rosenberg, B.; Camp, L. V.; Grimley, E. B.; Thomson, A. J. *J. Biol. Chem.* **1967**, *242*, 1347−1352.
(3) Clarke, M. J. *Met. Ions Biol. Syst.* **1980**, *11*, 231−283.
(4) (a) Süss-Fink, G. *Dalton Trans.* **2010**, *39*, 1673−1688. (b) Gasser, G.; Ott, I.; Metzler-Nolte, N. *J. Med. Chem.* **2011**, *54*, 3−25. (c) Gianferra, T.; Bratsos, I.; Alessio, E. *Dalton Trans.* **2009**, *2009*, 7588−7598.
(5) (a) Reedijk, J. *Proc. Natl. Acad. Sci. U.S.A.* **2003**, *100*, 3611−3613. (b) Guo, Z.; Sadler, P. J. *Angew. Chem., Int. Ed.* **1999**, *38*, 1512−1531. (c) Reedijk, J. *Platinum Met. Rev.* **2008**, *52*, 2−11.
(6) Renfrew, A. K.; Phillips, A. D.; Egger, A. E.; Hartinger, C. G.; Bosquain, S. S.; Nazarov, A. A.; Keppler, B. K.; Gonsalvi, L.; Peruzzini, M.; Dyson, P. J. *Organometallics* **2009**, *28*, 1165−1172.

(7) Hartinger, C. G.; Jakupec, M. A.; Zorbas-Seifried, S.; Groessl, M.; Egger, A.; Berger, W.; Zorbas, H.; Dyson, P. J.; Keppler, B. K. *Chem. Biodiversity* **2008**, *5*, 2140−2155.
(8) Rademaker-Lakhai, J. M.; van den Bongard, D.; Pluim, D.; Beijnen, J. H.; Schellens, J. H. M. *Clin. Cancer Res.* **2004**, *10*, 3717−3727.
(9) (a) Alessio, E.; Mestroni, G.; Nardin, G.; Attia, W. M.; Calligaris, M.; Sava, G.; Zorzet, S. *Inorg. Chem.* **1988**, *27*, 4099−4106. (b) Sava, G.; Pacor, S.; Zorzet, S.; Alessio, E.; Mestroni, G. *Pharmacol. Res.* **1989**, *21*, 617−628.
(10) (a) Bergamo, A.; Sava, G. *Dalton Trans.* **2007**, 1267−1272. (b) Hartinger, C. G.; Zorbas-Seifried, S.; Jakupec, M. A.; Kynast, B.; Zorbas, H.; Keppler, B. K. *J. Inorg. Biochem.* **2006**, *100*, 891−904.
(11) (a) Levina, A.; Mitra, A.; Lay, P. A. *Metallomics* **2009**, *1*, 458−470. (b) Ang, W. H.; Casini, A.; Sava, G.; Dyson, P. J. *J. Organomet. Chem.* **2011**, *696*, 989−998. (c) Antonarakis, E. S.; Emadi, A. *Cancer Chemother. Pharmacol.* **2010**, *66*, 1−9.
(12) (a) Clarke, M. J. *Coord. Chem. Rev.* **2002**, *232*, 69−93. (b) Yan, Y. K.; Melchart, M.; Habtemariam, A.; Sadler, P. J. *Chem. Commun.* **2005**, *38*, 4764−4776. (c) Wheate, N. J.; Brodie, C. R.; Collins, J. G.; Kemp, S.; Aldrich-Wright, J. R. *Mini-Rev. Med. Chem.* **2007**, *7*, 627−648.
(13) Bergamo, A.; Masi, A.; Dyson, P. J.; Sava, G. *Int. J. Oncol.* **2008**, *33*, 1281−1289.
(14) Matsumura, Y.; Maeda, H. *Cancer. Res.* **1986**, *46*, 6387−6392.
(15) Maeda, H. *Adv. Enzyme Regul.* **2001**, *41*, 189−207.
(16) Fox, M. E.; Szoka, F. C.; Frechet, J. M. J. *Acc. Chem. Res.* **2009**, *42*, 1141−1151.
(17) Fujita, M.; Yazaki, J.; Ogura, K. *J. Am. Chem. Soc.* **1990**, *112*, 5645−5646.
(18) (a) Pirondini, L.; Bertolini, F.; Cantadori, B.; Ugozzoli, F.; Massera, C.; Dalcanale, E. *Proc. Natl. Acad. Sci. U.S.A.* **2002**, *99*, 4911−4915. (b) Ovchinnikov, M. V.; Holliday, B. J.; Mirkin, C. A.; Zakharov, L. N.; Rheingold, A. L. *Proc. Natl. Acad. Sci. U.S.A.* **2002**, *99*, 4927−4931. (c) Kuehl, C. J.; Kryschenko, Y. K.; Radhakrishnan, U.; Russell Seidel, S.; Huang, S. D.; Stang, P. J. *Proc. Natl. Acad. Sci. U.S.A.* **2002**, *99*, 4932−4936. (d) Kryschenko, Y. K.; Russell Seidel, S.; Muddiman, D. C.; Nepomuceno, A. I.; Stang, P. J. *J. Am. Chem. Soc.* **2003**, *125*, 9647−9652. (e) Fujita, M.; Tominaga, M.; Hori, A.; Therrien, B. *Acc. Chem. Res.* **2005**, *38*, 369−378.
(19) (a) Rosi, N. L.; Eckert, J.; Eddaoudi, M.; Vodak, D. T.; Kim, J.; O'Keeffe, M.; Yaghi, O. M. *Science* **2003**, *300*, 1127−1129. (b) Yoshizawa, M.; Tamura, M.; Fujita, M. *Science* **2006**, *312*, 251−254. (c) Pluth, M. D.; Bergman, R. G.; Raymond, K. N. *Science* **2007**, *316*, 85−88. (d) Fujita, M.; Oguro, D.; Miyazawa, M.; Oka, H.; Yamaguchi, K.; Ogura, K. *Nature* **1995**, *378*, 469−471.
(20) (a) Therrien, B.; Süss-Fink, G.; Govindaswamy, P.; Renfrew, A. K.; Dyson, P. J. *Angew. Chem., Int. Ed.* **2008**, *47*, 3773−3776. (b) Barry, N. P. E.; Zava, O.; Furrer, J.; Dyson, P. J.; Therrien, B. *Dalton Trans.* **2010**, *39*, 5272−5277. (c) Mattson, J.; Govindaswamy, P.; Renfrew, A. K.; Dyson, P. J.; Štěpnička, P.; Süss-Fink, G.; Therrien, B. *Organometallics* **2009**, *28*, 4350−4357. (d) Therrien, B. *Eur. J. Inorg. Chem.* **2009**, 2445−2453. (e) Vajpayee, V.; Yang, Y. J.; Kang, S. C.; Kim, H.; Kim, I. S.; Wang, M.; Stang, P. J.; Chi, K. W. *Chem. Commun.* **2011**, *47*, 5184−5186. (f) Vajpayee, V.; Song, Y. H.; Yang, Y. J.; Kang, S. C.; Kim, H.; Kim, I. S.; Wang, M.; Stang, P. J.; Chi, K. W. *Organometallics* **2011**, *30*, 3242−3245.
(21) Ang, W. H.; Grote, Z.; Scopelliti, R.; Juillerat-Jeanneret, L.; Severin, K.; Dyson, P. J. *J. Organomet. Chem.* **2009**, *694*, 968−972.
(22) Wang, M.; Vajpayee, V.; Shanmugaraju, S.; Zheng, Y.-R.; Zhao, Z.; Kim, H.; Mukherjee, P. S.; Chi, K.-W.; Stang, P. J. *Inorg. Chem.* **2011**, *50*, 1506−1512.
(23) Govindaswamy, P.; Süss-Fink, G.; Therrien, B. *Organometallics* **2007**, *26*, 915−924.
(24) (a) Govindaswamy, P.; Furrer, J.; Süss-Fink, G.; Therrien, B. *Z. Anorg. Allg. Chem.* **2008**, *634*, 1349−1352. (b) Mattsson, J.; Govindaswamy, P.; Furrer, J.; Sei, Y.; Yamaguchi, K.; Süss-Fink, G.; Therrien, B. *Organometallics* **2008**, *27*, 4346−4356. (c) Barry, N. P. E.; Therrien, B. *Eur. J. Inorg. Chem.* **2009**, 4695−4700. (d) Freudenreich, J.; Barry, N. P. E.; Süss-Fink, G.; Therrien, B. *Eur. J. Inorg. Chem.* **2010**, 2400−2405. (e) Mattsson, J.; Zava, O.; Renfrew, A. K.; Sei, Y.; Yamaguchi, K.; Dyson, P. J.; Therrien, B. *Dalton Trans.* **2010**, *39*, 8248−8255. (f) Zava, O.; Mattsson, J.; Therrien, B.; Dyson, P. J. *Chem.—Eur. J.* **2010**, *16*, 1428−1431.
(25) Hwang, T. L.; Shaka, A. J. *J. Am. Chem. Soc.* **1992**, *114*, 3157−3159.
(26) (a) Morris, G. A. In *Encyclopedia of Nuclear Magnetic Resonance*; Wiley: New York, 2002; Vol. *9*, pp 35-44. (b) Morris, K. F.; Johnson, C. S. *J. Am. Chem. Soc.* **1992**, *114*, 3139−3141.
(27) (a) Glasoe, P. K.; Long, F. A. *J. Phys. Chem.* **1960**, *64*, 188−189. (b) Mikkelsen, K.; Nielsen, S. O. *J. Phys. Chem.* **1960**, *64*, 632−637.
(28) (a) Clarke, M. J.; Zhu, F.; Frasca, D. R. *Chem. Rev.* **1999**, *99*, 2511−2533. (b) Allardyce, C. S.; Dyson, P. J. *Platinum Met. Rev.* **2001**, *45*, 62−69. (c) Timerbaev, A. R.; Hartinger, C. G.; Aleksenko, S. S.; Keppler, B. K. *Chem. Rev.* **2006**, *106*, 2224−2248. (d) Jakupec, M. A.; Galanski, M.; Arion, V. B.; Hartinger, C. G.; Keppler, B. K. *Dalton Trans.* **2008**, *2008*, 183−194. (e) Hartinger, C. G.; Keppler, B. K. *Electrophoresis* **2007**, *27*, 3436−3446.
(29) Nishikawa, Y.; Kurata, T. *Biosci. Biotechnol. Biochem.* **2000**, *64*, 476−483.
(30) Wang, Y. N.; Lau, K. C.; Lam, W. W. Y.; Man, W. L.; Leung, C. F.; Lau, T. C. *Inorg. Chem.* **2009**, *48*, 400−406.
(31) Sava, G.; Bergamo, A.; Zorzet, S.; Gava, B.; Casarsa, C.; Cocchietto, M.; Furlani, A.; Scarcia, V.; Serli, B.; Iengo, E.; Alessio, E.; Mestroni, G. *Eur. J. Cancer* **2002**, *38*, 427−435.
(32) (a) Sheldrick, W. S.; Heeb, S. *J. Organomet. Chem.* **1989**, *377*, 357−366. (b) Sheldrick, W. S.; Exner, R. *Inorg. Chim. Acta* **1992**, *195*, 1−9.
(33) Wang, F.; Chen, H.; Parkinson, J. A.; Murdoch del Socorro, P.; Sadler, P. J. *Inorg. Chem.* **2002**, *41*, 4509−4523.
(34) Krämer, R.; Maurus, M.; Bergs, R.; Polborn, K.; Sünkel, K.; Wagner, B.; Beck, W. *Chem. Ber.* **1993**, *126*, 1969−1980.
(35) (a) Ivanov, A. I.; Christodoulou, J.; Parkinson, J. A.; Barnham, K. J.; Tucker, A.; Woodrow, J.; Sadler, P. J. *J. Biol. Chem.* **1998**, *273*, 14721−14730. (b) Hahn, M.; Kleine, M.; Sheldrick, W. S. *J. Biol. Inorg. Chem.* **2001**, *6*, 556−566. (c) Esposito, B. P.; Najjar, R. *Coord. Chem. Rev.* **2002**, *232*, 137−149. (d) Arnesano, F.; Scintilla, S.; Natile, G. *Angew. Chem., Int. Ed.* **2007**, *46*, 9062−9064.
(36) Ivanova, B. B.; Mitewa, M. I. O. *J. Coord. Chem.* **2004**, *57*, 271−221.
(37) Hanif, M.; Henke, H.; Meier, S. M.; Martic, S.; Labib, M.; Kandioller, W.; Jakupec, M. A.; Arion, V. B.; Kraatz, H.-B.; Keppler, B. K.; Hartinger, C. G. *Inorg. Chem.* **2010**, *49*, 7953−7963.
(38) Sharma, D.; Rajarathnam, K. *J. Biomol. NMR* **2000**, *18*, 165.
(39) Meister, A.; Anderson, M. E. *Annu. Rep. Biochem.* **1983**, *52*, 711.
(40) Dougan, S. J.; Habtemariam, A.; McHale, S. E.; Parsons, S.; Sadler, P. J. *Proc. Natl. Acad. Sci. U.S.A.* **2008**, *105*, 11628.
(41) Giannini, F.; Süss-Fink, G.; Furrer, J. *Inorg. Chem.* **2011**, *50*, 10552−10554.
(42) Nakayama, T.; Isobe, T.; Nakamyiya, K.; Edmonds, J. S.; Shibata, Y.; Morita, M. *Magn. Reson. Chem.* **2005**, *43*, 543.
(43) Sugio, S.; Kashima, A.; Mochizzki, S.; Noda, M.; Kobayashi, K. *Protein Eng.* **1999**, *12*, 439−446.
(44) Ohta, T.; Nakahara, S.; Shigemura, Y.; Hattori, K.; Furukawa, I. *Appl. Organomet. Chem.* **2001**, *15*, 699−709.
(45) (a) Govindaswamy, P.; Süss-Fink, G.; Therrien, B.; Štěpnička, P.; Ludvík, J. *J. Organomet. Chem.* **2007**, *692*, 1661−1671. (b) Thai, T.-T.; Therrien, B.; Süss-Fink, G. *J. Organomet. Chem.* **2009**, *694*, 3973−3981. (c) Govender, P.; Renfrew, A.; Clavel, C. M.; Dyson, P. J.; Therrien, B.; Smith, G. S. *Dalton Trans.* **2011**, *40*, 1158−1167.
(46) Stodt, R.; Gencaslan, S.; Muller, I. M.; Sheldrick, W. S. *Eur. J. Inorg. Chem.* **2003**, *10*, 1873−1882.